5/20/66

A

NASA CONTRACTOR REPORT

NASA CR-471

NASA CR-471

A SEMI-ATOMISTIC MODEL FOR FLAW-INDUCED FRACTURE IN NON-DUCTILE MATERIALS

by H. Schuerch

Prepared under Contract No. NASw-652 *by*
ASTRO RESEARCH CORPORATION
Santa Barbara, Calif.
for

NATIONAL AERONAUTICS AND SPACE ADMINISTRATION • WASHINGTON, D. C. • MAY 1966

TABLE OF CONTENTS

ABSTRACT

A semi-atomistic model is proposed for the non-ductile failure of materials based upon an analysis of static and dynamic stress concentrations in uniaxial fiber-matrix composite materials. In this model the finite spacing of bonds is accounted for in the direction of a crack or flaw, while the material is considered as continuous in the perpendicular direction. An elementary, two-dimensional analysis based on linear force-displacement laws shows, that the stress concentration is dependent only upon the digital quantity of the number of adjacent, broken filaments or bonds, and is independent of the spacing and of the relative elastic properties of the fiber and matrix. The form of the static stress concentration factor

$$K_n = \sqrt{\frac{\pi}{2}}\sqrt{n} = \sqrt{\frac{\pi}{2}}\sqrt{\frac{c}{d}}$$

where n is the number of adjacent broken bonds, c is the crack depth and d is the bond spacing, is formally equivalent to that obtained using relations given by Griffith (Ref. 1) and Charles (Ref. 3).

The results of the elementary analysis are of sufficient significance to warrant extension of the theory to non-linear force elongation, and to account for temperature, stress corrosion and static fatigue effects. In addition, experimental verification of this theory should be undertaken using both covalent and ionically bonded materials, as well as metals under conditions where non-ductile failure occurs.

I. INTRODUCTION

The technical strength of non-ductile materials has become of increasing interest because of their use in fibers (glass, elemental boron, oxides, carbides, etc.) and thermosetting polymers (epoxies, silicones, polybenzimidazoles, etc.) that form the constituents of many high performance composites used in advanced structural applications. Further, many methods of improving the tensile strength of metallic materials do so by reducing dislocation mobility and tend towards generating non-ductile fracture modes. Also, the use of refractory oxide ceramics, carbides, graphite and carbon in bulk shapes for structural applications forces attention upon their essentially non-ductile failure phenomena.

Other reasons for interest in the strength and failure of non-ductile materials are found in cryogenic applications. In these applications, elastomeric or thermoplastic materials are often forced to operate at temperatures below the "glass transition", where they exhibit brittle, non-ductile fracture associated with catastrophic crack propagation.

II. INTRINSIC AND TECHNICAL STRENGTH OF MATERIALS

Solids derive their resistance to deformation from three types of interatomic bonds:

- metallic,
- ionic, and
- covalent.

A schematic representation of the force-deformation characteristic inherent in the interatomic bond is shown in Figure 1.

Conventional materials of construction are predominantly metallic. Metals exhibit dislocation mobility, which allows the relief of stress concentration by what is, in effect, a premature but non-catastrophic (i.e., "self-healing") failure mode. A general term for this type of materials response to stress is "ductility". Even metallic materials, however, may exhibit non-ductile fracture where impurities, work hardening and cyclic fatigue (dislocation pile-up), or peculiar crystallographic properties (beryllium) restrict dislocation mobility.

Other types of materials derive their cohesion from electrostatic forces (ionic bonds) and from quantum mechanical electron exchange forces (covalent bonds). The latter bonds are typical for ceramics, glasses, etc. Because covalent bonding forces are space oriented they usually prevent dislocation motion, and therefore, in principle, can provide materials of much higher strength.

However, because of the absence of the "ductile" stress relief mechanism possible for metallic (and some ionic) bonds, covalently bonded materials are subject to other premature failure modes that are associated with either static or dynamic stress concentrations (brittle fracture).

The observed tensile strength of non-ductile materials is orders of magnitude lower than the intrinsic interatomic cohesion that can be derived, for instance, from their heat of sublimation. Following original work of Griffith, Inglis, and others (Refs. 1-3) explanations for this deficiency have been given in terms of observed or postulated flaws that are responsible for microscopic stress concentrations in a seemingly uniformly stressed body.

One unsatisfactory aspect of the classical flaw theory is its dependence upon an isotropic, continuous medium for calculation of the stress at the crack tip and the necessity to postulate a finite crack tip radius to obtain finite values for stress concentration factors. Equally unsatisfactory are treatments involving a free-surface energy or "surface tension" and related potential energy postulates to determine critical flaw size. The first approach obviously violates the discrete nature of molecular arrangements that must be considered in an atomistic view of the crack tip geometry. The second approach deals with the static situation prevailing at some time after the failure has occurred, and is

incapable of accounting for the detailed dynamic mechanisms attending the straining and failure of interatomic bonds. (A portion of the failure energy must leave the failure domain in the form of thermoelastic wavelets or phonons.)

An attempt to account for finite bond spacing has been presented by Elliot (Ref. 4). Here the material was considered as a Hookean elastic continuum with the exception of two monatomic layers immediately adjoining the crack area. This concept allows accounting for the non-linear force-elongation characteristics of highly strained bonds, but suffers from the transition to continuum mechanics at an atomic distance removed from the crack. For instance, analysis of cohesive force distribution based on Elliot's model yields large stress gradients in distances smaller than the interatomic spacing. This result is difficult to reconcile with the discrete nature of materials.

A new approach, suggested by the results of a recent study on crack propagation in filamentary materials with partially broken filaments (Ref. 5), avoids the necessity of postulating crack tip radii, but retains an essentially continuum mechanical approach suitable for analytical treatment. As applied to interatomic dimensions this approach provides a semi-atomistic model in the sense that finite spacing of bonds is accounted for in the direction of the crack, while the material is considered as continuous in the

direction perpendicular to the crack. This concept is developed here for the prediction of flaw effects on technical strength, and is correlated with published experimental data. Extension of this theory to non-linear force-elongation, and to account for temperature effects, stress corrosion, static fatigue, etc., is possible in principle, but has not been carried out in detail.

III. FRACTURE ANALYSIS

Hedgepeth (Ref. 5) has treated the case of a one-dimensional array of parallel elastic filaments in a matrix with elastic shearing stiffness, and with a crack extending over n filaments, as shown in Figure 2. The array is assumed to be subject to uniaxial tension in a direction normal to the crack. The static stress concentration factor, K_n, for the first unbroken filament is given by the recursion formula

$$K_n = \frac{4 \cdot 6 \cdot 8 \quad (2n + 2)}{3 \cdot 5 \cdot 7 \quad (2n + 1)} \tag{1}$$

Figure 3 shows the relation between the number of broken filaments, n, and the stress concentration factor, as given in Equation 1. K_n diverges for large n, but can be represented with high accuracy for $n > 10$ by

$$K_n = \frac{\sqrt{\pi}}{2}\sqrt{n} \quad \exp\left(\frac{5}{8n}\right) \tag{2}*$$

Since $\exp\left(\frac{5}{8n}\right)$ converges rapidly to unity for large n, Equation 2 can also be approximated by

$$K_n \approx \frac{\sqrt{\pi}}{2}\sqrt{n} \tag{2a}$$

* The derivation of this expression is due to G. Schindler and is given in Appendix A.

It is significant that, within the limitations of the analysis, the stress concentration is independent of the spacing and of the elastic properties of fiber and matrix, and is dependent only on a digital quantity, i.e., the number of adjacent broken filaments.

It is further interesting that the form of the stress concentration factor given in Equation 2a is formally equivalent to that which can be obtained by using relations given by Griffith (Ref. 1) and by Charles (Ref. 3) for the critical stress at failure σ_{cr}, and for the intrinsic strength, F, respectively:

$$\sigma_{cr} = \sqrt{4 \frac{SE}{\pi c}} \tag{3}$$

and

$$F = \sqrt{\frac{SE}{a}} \tag{4}$$

where S is the surface energy, E is the Young's modulus, c is the crack depth, and a is the interatomic spacing.

Combining Equations (3) and (4) yields

$$K_n = F \Big/ \sigma_{cr} = \frac{\sqrt{\pi}}{2} \sqrt{\frac{c}{a}} \tag{5}$$

In addition to the static stress concentration described by Equation 1, dynamic overload stresses occur due to the elastic waves generated by the sudden fracture of one or several filaments. The dynamic overload, η_k, due to a sudden fracture of k filaments

is given by Hedgepeth (Ref. 5) for 1, 2, 3 filaments as 1.15, 1.19 and 1.20, respectively, with a limiting value of $\eta_\infty = 1.27$ for the simultaneous failure of many filaments.

This analysis assumes that k filaments fail simultaneously, but that prior to the failure all filaments were intact. The results of this analysis can also be used as a first approximation to the case where pre-existing failures have generated a static crack, and where the instantaneous failure of k additional filaments produce a dynamic stress concentration.

Consider now a non-ductile material with a "flaw" in the form of a plane region perpendicular to the direction of applied stress, as shown in Figure 4. The flaw may either be at the surface or in the interior of the body.

We may now use the concept of "filaments" for the arrays of molecular bonds in the direction of the applied stress. A plane section parallel to the axis of stress, and passing through the maximum diameter of the flaw, may then exhibit a picture very much like the two-dimensional array of filaments shown in Figure 2. The stress concentration prevailing in the bonds adjacent to the flaw edge is given by Equation 1 or 2, and is seen to depend solely on the number of broken bonds, $n = 2c/d$. In this equation 2c is the maximum diameter of the interior flaw (or, c is the depth of a surface flaw), and d is the spacing of the broken bonds, measured

in the plane of the flaw. With this semi-atomistic model, the critical stress level at which crack propagation will occur becomes, for large n,

$$\sigma_{cr} = \frac{F}{\eta_k K_n} = \frac{2F}{\eta_k \sqrt{\pi n}} \qquad (6)$$

It is seen that, according to this analysis, failure will occur at a fraction of the intrinsic strength, and that this fraction is dependent both on the number of broken bonds in the pre-existing flaw, and on the nature of the micro-dynamic stress concentration caused by sudden additional bond fracture.

IV. DISCUSSION OF MICRO-DYNAMIC EFFECTS

We may distinguish three mechanisms of crack-propagation, depending upon severity of the dynamic effect:

a) Quasi-static (Creeping) Crack Propagation

Crack propagation is thermochemically activated, i.e., the elastic wave (phonon-packet) emitted by the failure of a single bond is insufficient to cause immediate failure of additional bonds. The static stress concentration is high enough, however, that after sufficient elapsed time, failure will occur by chemical attack of adsorbed atmospheric constituents (particularly of water in the case of silica glasses) and, possibly, by random thermal motion. This process is similar to that which can be postulated for surface solubility and sublimation of solids except that the bond failure probability here is enhanced by the mechanically induced bond strain at the crack tip. These effects will reduce the intrinsic bond strength, but, in this case, the "dynamic stress concentration" can be neglected.

b) Transition

There is a threshold case where the transient stress concentration of the bond failure process is sufficient to cause failure of the adjacent bond before the dynamic

stress has dissipated, but with sufficient time delay to prevent the catastrophic interaction of phonons emitted by consecutive failures. The speed of crack propagation will be expected to be small compared to the velocity of sound in the material. Dynamic overload factors of the order of those given in Reference 5 for single instantaneous bond failure will be expected.

c) Catastrophic Crack Propagation

Crack propagation is "instantaneous" in the sense that the dynamic effect of a large number of bond failures will accumulate causing the bond at the crack tip to fail without thermal delay. Thus, a shock wave will be generated that will be expected to propagate at sonic velocity.

V. EXPERIMENTAL CORRELATION

Experiments concerning the tensile strength of glass with flaws or initial cracks of various sizes and origins have been reported by many investigators. The absolute values of measured strength vary over a wide range depending on conditions of test, size and shape of test specimens, atmosphere, aging, previous heat treatments of glass (temper), etc. It is found by many investigators, however, that the measured strength is inversely proportional to the square root of the flaw size, as predicted by Equation 6. Also, a marked dependency of failure strength with rate of load application, "static fatigue", and slow growth of cracks that are originally smaller than the critical size, has been well established. These observations correlate qualitatively with the dynamic failure model discussed here.

The theoretical critical bond failure number n, given by Equation 6, is plotted vs σ_{cr} /F in Figure 5, using Hedgepeth's "two-dimensional" dynamic factors of 1.15 and 1.27 for transition and catastrophic crack propagation, respectively, and using 1.0 for the quasi-static case of "creeping" crack propagation. Also plotted in Figure 5 are data from Reference 1 (for relatively large cracks) and Reference 4 (for small surface abrasions) for comparison between the present theory and experiments.

For the purpose of this comparison, several assumptions were made:

1. The bond spacing d was assumed to be the inverse square root of the number of Si-0 bonds/unit area in fused silica (Ref. 3) yielding

$$d = 5.4 \text{ Å} = 2.1 \times 10^{-8} \text{ in.}$$

We note that this value is considerably larger than the Si-0 bond distance

$$a_{Si-0} = 1.6 \text{ Å} = .63 \times 10^{-8} \text{ in.}$$

The reason for this difference becomes evident if the open network-structure of silica shown schematically in Figure 6 is considered.

2. The intrinsic strength was assumed to be 2.5×10^6 psi for glass tested in normal atmosphere (tests by Griffith, Ref. 1) 1.8×10^6 psi and 3.2×10^6 psi for tests in water and in liquid nitrogen, respectively (tests by Mould and Southwick, Ref. 6). The value of 2.5×10^6 psi correlates well with experimental values obtained from thin, presumably flaw-free filaments (Ref. 3), and with the theoretical strength obtained from Equation 4, if the bond distance, a, is replaced by the bond spacing d = 5.4 Å. The increase of intrinsic strength due to immersion in liquid nitrogen

may be correlated to two factors: The lower temperature reduces thermal activation of the failure mechanism itself. Also, the lower temperature will reduce chemical attack of the fracture tip with attendant lowering of the residual intrinsic bond strength such as observed in the tests conducted immersed in water.

VI. CONCLUSIONS AND RECOMMENDATIONS

The semi-atomistic model of non-ductile failure appears to predict the essential features of failure observed in glassy materials. The analysis here has been restricted to a two-dimensional model and has not accounted for the detailed mechanisms attending an intermolecular bond failure. This refinement is, however, possible in principle and should yield a more complete understanding of failure mechanics on an atomic level. Two particular subjects should be considered:

- A theoretical treatment of the dynamic failure phenomena, including consideration of thermal vibrations, and
- An expansion of Hedgepeth's work to include three-dimensional arrays of bonds, as well as network-structures of the type shown in Figure 5, and to include realistic non-linear force displacement characteristics of the intermolecular bond.

Well controlled static and dynamic fracture experiments with non-ductile materials of current technical interest, including artificially induced flaws in the test specimens should be conducted to correlate refined theoretical predictions. Such experiments should be conducted first in inert atmospheres to eliminate the obscuring effects of chemical crack tip attack. Later, both theoretical and experimental work should be devoted to a quantitative

understanding of "stress-corrosion" as it affects catastrophic and creeping crack growth.

Candidate materials for such experimental studies are refractory metals, thermosetting polymers, thermoplastics and elastomers at temperatures below the glass transition, and "exotic" polycrystalline or amorphous materials such as boron, beryllium, carbon and graphites in either bulk or fiber form.

REFERENCES

1. Griffith, A. A., "The Phenomena of Rupture and Flow in Solids", Trans. Roy. Soc., London, A.221, 163-98 (1920).

2. Inglis, C. E., "Stresses in a Plate Due to the Presence of Cracks and Sharp Corners", Trans. Inst. Nav. Architects, London, 55 219-242 (1913).

3. Charles, R. J., "A Review of Glass Strength" from the book: Fracture of Solids, John Wiley and Sons, Inc., New York, pp. 1-38 (1963).

4. Elliot, H. A., "An Analysis of the Conditions for Rupture Due to Griffith Cracks", Proc. Phys. Soc. 59, 208 (1947).

5. Hedgepeth, J. M., "Stress Concentrations in Filament Structures", NASA TN D-882, May 1961.

6. Mould, R. E., Southwick, R. P., "Strength and Static Fatigue of Abraded Glass", J. Amer. Ceram. Soc., 42 582-92 (1959).

7. Knopp, K., "Theory and Application of Infinite Series", Hafner Publishing Company, New York.

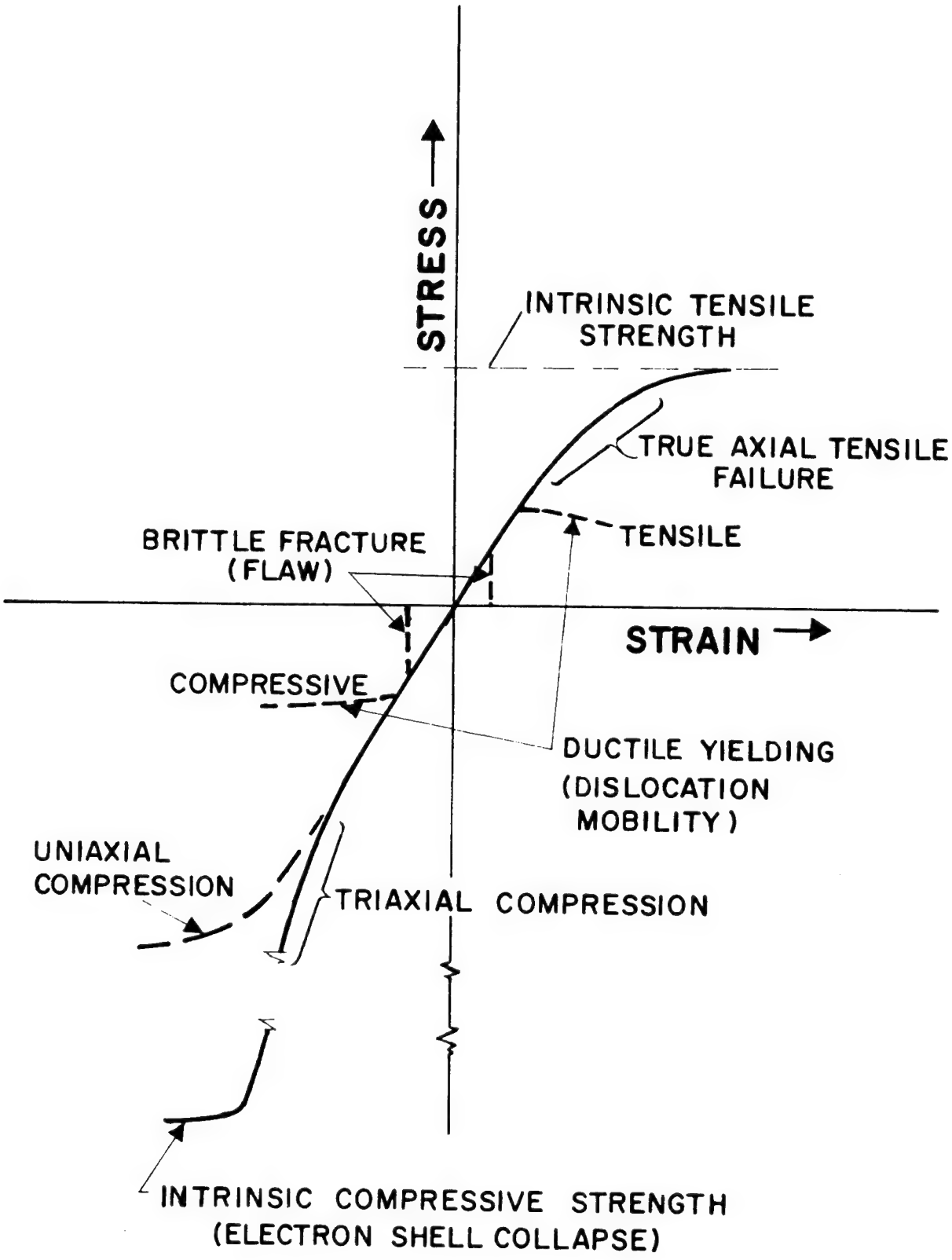

FIG. I: INTRINSIC STRENGTH OF MATERIALS

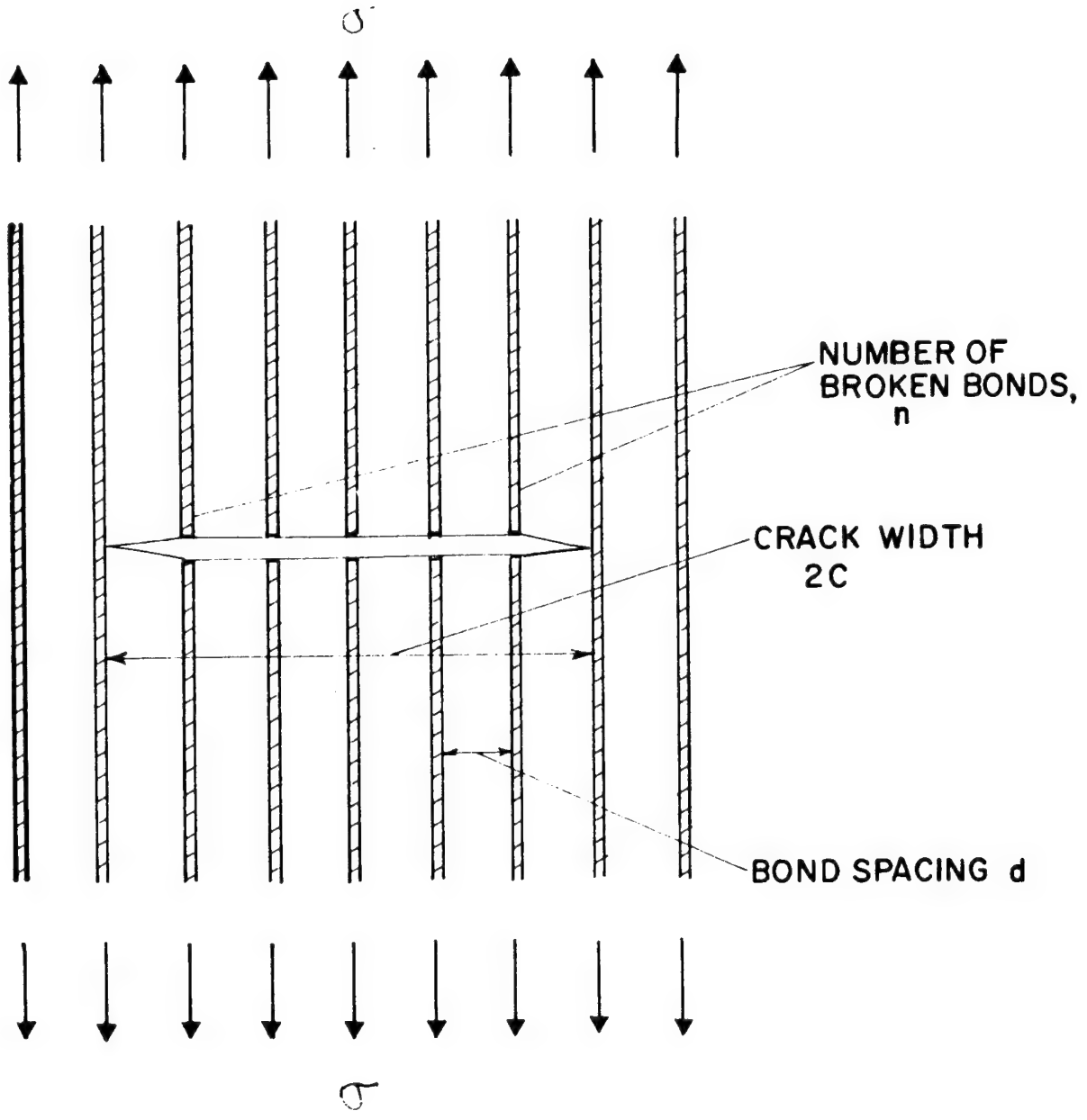

FIG. 2: PARTIALLY CRACKED UNIFORM ARRAY OF BONDS

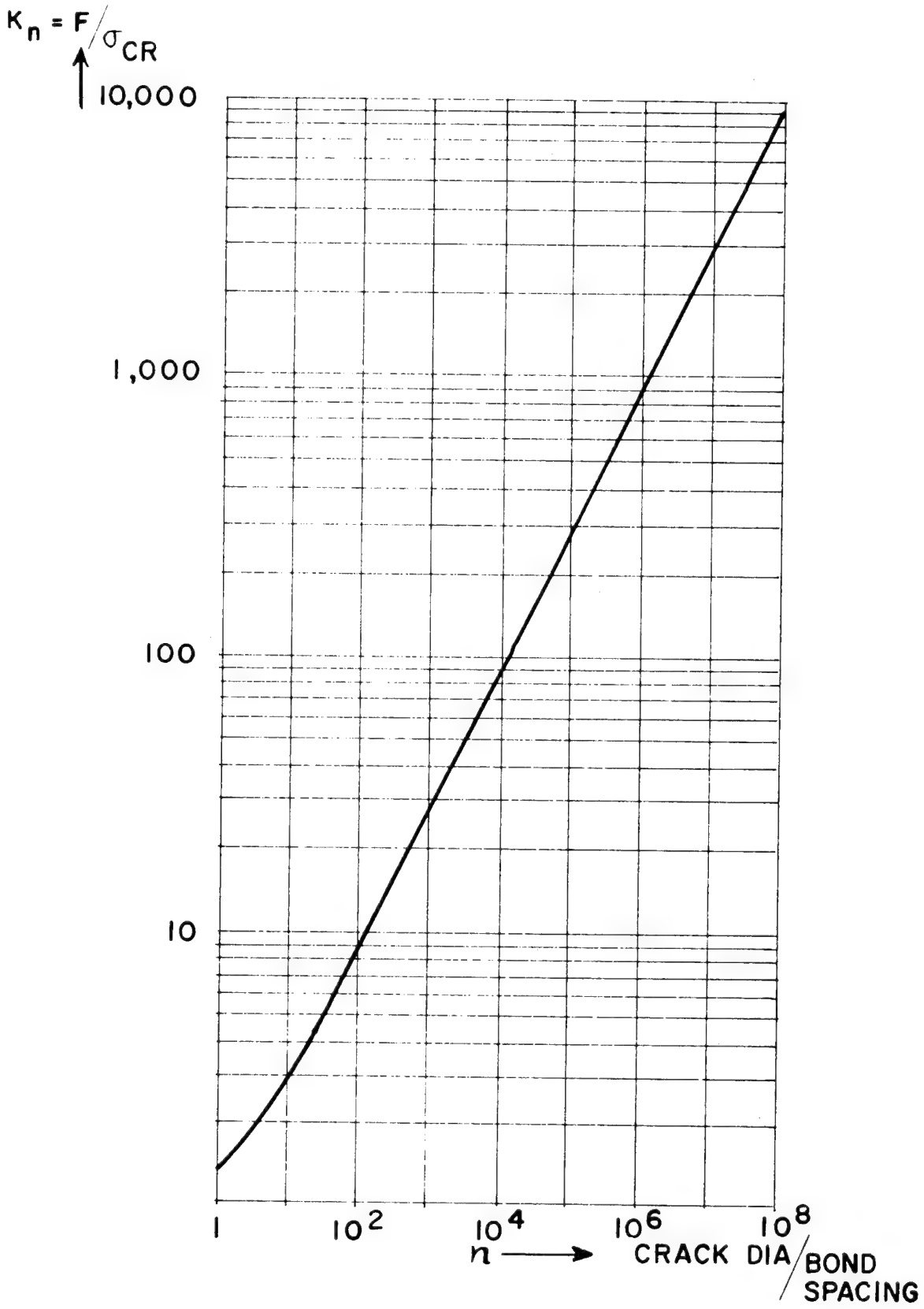

FIG. 3 : RATIO OF THEORETICAL AND TECHNICAL STRENGTH VS NUMBER OF BROKEN BONDS

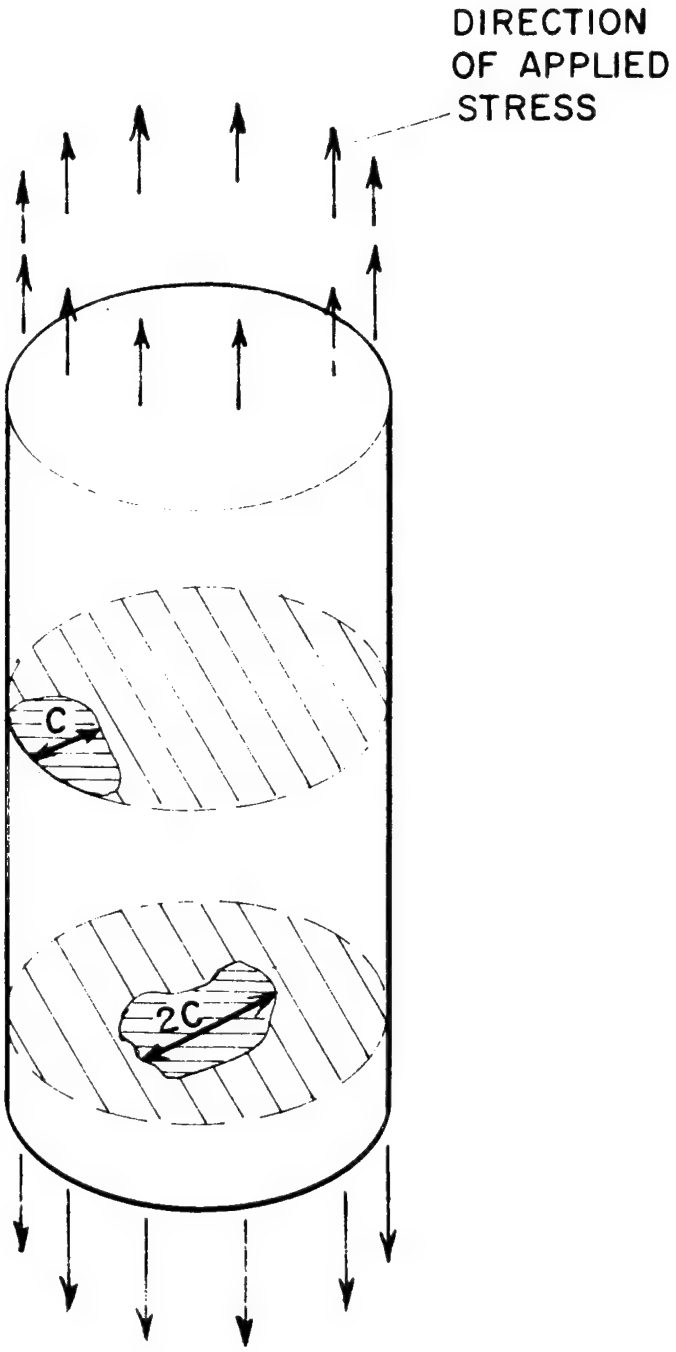

FIG. 4: FLAWS IN BRITTLE MATERIAL

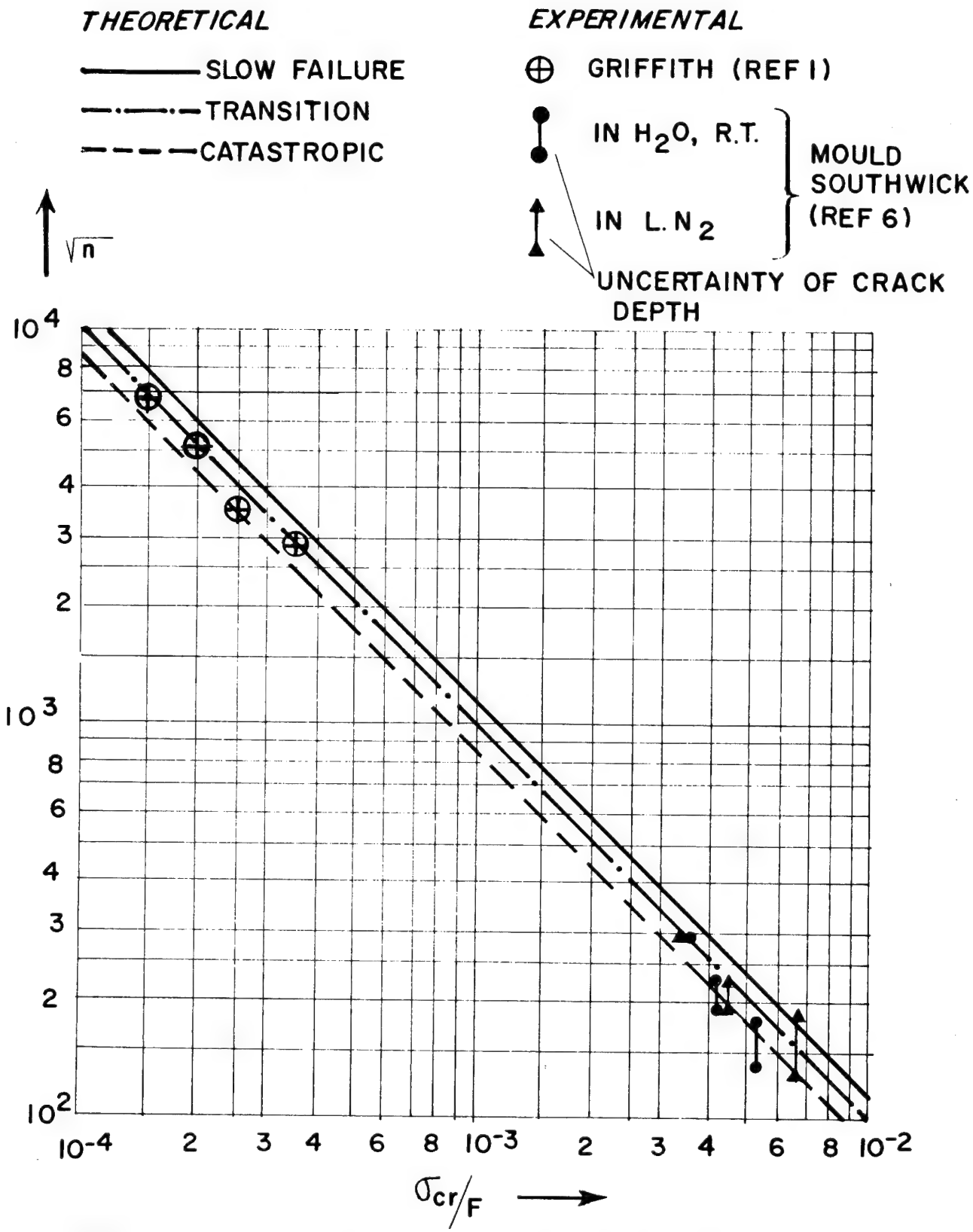

FIG. 5: CRITICAL BOND FAILURE COUNT VS. STRESS AT FAILURE - THEORY AND EXPERIMENT

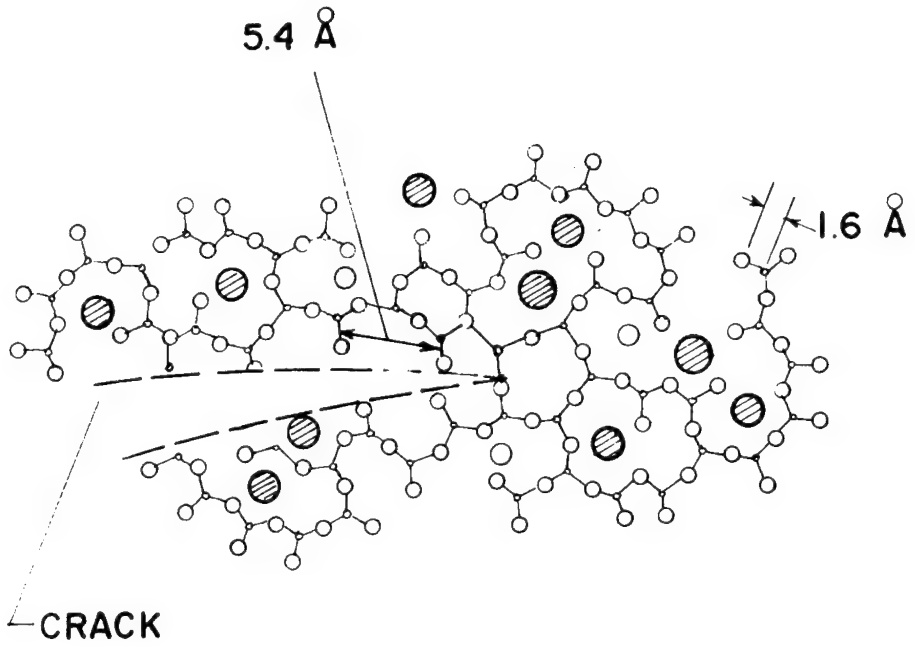

FIG. 6: SCHEMATIC REPRESENTATION OF GLASSY NETWORK STRUCTURE WITH CRACK

APPENDIX

Reference 5 determined the stress concentration factor, K_n, for a plane filamentary structure in the static equilibrium in the case of n broken filaments as follows:

$$K_n = \frac{4 \cdot 6 \cdot 8 \cdots (2n+2)}{3 \cdot 5 \cdot 7 \cdots (2n+1)} \tag{A-1}$$

For large n, expression A-1 is inconvenient to evaluate. Equation A-1 can be written

$$K_n = 2^{2n} \frac{n!\,(n+1)!}{(2n+1)!} \tag{A-2}$$

According to Reference 7, the quantity n! can be expressed in the form

$$n! = \sqrt{2\pi}\; n^{\left(n+\frac{1}{2}\right)} \cdot e^{\left(-n+A_n\right)} \tag{A-3}$$

where

$$A_n = \int_n^{\infty} \frac{1}{x} \sum_{r=1}^{\infty} \frac{\sin 2\pi r x}{r\pi}\, dx \tag{A-4}$$

Inserting (A-3) into (A-2), one obtains

$$K_n = \frac{1}{2}\sqrt{\pi n} \cdot \frac{\left(1+\frac{1}{n}\right)^{n+\frac{3}{2}}}{\left(1+\frac{1}{2n}\right)^{2n+\frac{3}{2}}} \cdot e^{\left(A_n+A_{n+1}-A_{2n+1}\right)} \tag{A-5}$$

Forming the natural logarithm of this expression, it follows that

$$\log K_n = \frac{1}{2}\log\left(\frac{\pi n}{4}\right) + \left(n+\frac{3}{2}\right)\log\left(1+\frac{1}{n}\right) - \left(2n+\frac{3}{2}\right)\log\left(1+\frac{1}{2n}\right) +$$

$$\left(A_n + A_{n+1} - A_{2n+1}\right) \qquad \text{(A-6)}$$

If $n \geq 1$, the expressions $\log\left(1+\frac{1}{n}\right)$ and $\log\left(1+\frac{1}{2n}\right)$ can be written in a power series

$$\log\left(1+\frac{1}{n}\right) = \frac{1}{n} - \frac{1}{2}\cdot\frac{1}{n^2} + \frac{1}{3}\cdot\frac{1}{n^3} \mp \cdots = \sum_{r=1}^{\infty}(-1)^{r-1}\frac{1}{r}\cdot\left(\frac{1}{n}\right)^r$$

$$\log\left(1+\frac{1}{2n}\right) = \frac{1}{2n} - \frac{1}{2}\cdot\frac{1}{(2n)^2} + \frac{1}{3}\cdot\frac{1}{(2n)^3} \mp \cdots = \sum_{r=1}^{\infty}(-1)^{r-1}\cdot\frac{1}{r}\cdot\left(\frac{1}{2n}\right)^r$$

After some transformations we obtain

$$\left(n+\frac{3}{2}\right)\log\left(1+\frac{1}{n}\right) - \left(2n+\frac{3}{2}\right)\log\left(1+\frac{1}{2n}\right) =$$

$$\frac{1}{2n} + \frac{1}{2}\cdot\frac{1}{(2n)^2}\cdot B_n \qquad \text{(A-7)}$$

Inserting (A-7) into (A-6) yields

$$\log K_n = \frac{1}{2}\log\left(\frac{\pi n}{4}\right) + \frac{1}{2n} + \frac{1}{2}\cdot\frac{1}{(2n)^2}\,B_n + \left(A_n + A_{n+1} - A_{2n+1}\right) \qquad \text{(A-8)}$$

According to Equation (A-7), the series for B_n can be majorized as follows:

$$\left|B_n\right| \leq \left|\sum_{r=0}^{\infty} 1 \cdot \left[4\left(\frac{1}{n}\right)^r - \left(\frac{1}{2n}\right)^r\right]\right| \leq 4 \sum_{r=0}^{\infty}\left(\frac{1}{n}\right)^r = \frac{4}{1-\frac{1}{n}} \qquad \text{(A-9)}$$

Equation (A-4) yields after integration by parts:

$$A_n = \frac{2}{n} \sum_{r=1}^{\infty} \frac{1}{4\pi^2 \cdot r^2} - 4 \int_n^{\infty} \frac{1}{x^3} \sum_{r=1}^{\infty} \frac{\sin 2\pi r x}{(2\pi r)^3}\, dx \qquad \text{(A-10)}$$

Now, according to Reference 7,

$$\sum_{r=1}^{\infty} \frac{1}{r^2} = \frac{\pi^2}{6}$$

$$0 < \sum_{r=1}^{\infty} \frac{1}{r^3} < \sum_{r=1}^{\infty} \frac{1}{r^2} = \frac{\pi^2}{6} \qquad \text{(A-11)}$$

Hence:

$$A_n = \frac{1}{12} \cdot \frac{1}{n} - C_n =$$

$$\frac{1}{12} \cdot \frac{1}{n} - 4 \int_n^{\infty} \frac{1}{x^3} \cdot \sum_{r=1}^{\infty} \frac{\sin 2\pi r x}{(2\pi r)^3}\, dx \qquad \text{(A-12)}$$

The sum $\left(A_n + A_{n+1} - A_{2n+1}\right)$ can be expressed as follows:

$$A_n + A_{n+1} - A_{2n+1} = \frac{1}{12}\left[\frac{1}{n} + \frac{1}{n+1} - \frac{1}{2n+1}\right] -$$

$$\left(C_n + C_{n+1} - C_{2n+1}\right) \qquad \text{(A-13)}$$

The remainder can be estimated by

$$\left| C_n + C_{n+1} - C_{2n+1} \right| \leq 4 \cdot 3 \int_n^\infty \frac{1}{x^3} \sum_{r=1}^\infty \frac{1}{(2\pi r)^3} \, dx \leq$$

$$\frac{3}{2\pi^3} \cdot \sum_{r=1}^\infty \frac{1}{r^2} \int_n^\infty \frac{1}{x^3} \, dx = \frac{1}{8\pi} \cdot \frac{1}{n^2} \qquad \text{(A-14)}$$

It is further for $n > 0$:

$$\frac{1}{n+1} = \frac{1}{n} - \frac{1}{n^2} \cdot \frac{1}{\left(1+\frac{1}{n}\right)}$$

and

(A-15)

$$\frac{1}{2n+1} = \frac{1}{2n} - \frac{1}{(2n)^2} \frac{1}{\left(1 + \frac{1}{2n}\right)}$$

Hence, Equation (A-13) reads

$$A_n + A_{n+1} - A_{2n+1} =$$

$$\frac{1}{8} \cdot \frac{1}{n} - \frac{1}{12} \left[\frac{1}{\left(1 + \frac{1}{n}\right)} - \frac{1}{4} \cdot \frac{1}{\left(1 + \frac{1}{2n}\right)} \right] \cdot \frac{1}{n^2} - \left(C_n + C_{n+1} \; C_{2n+1} \right)$$

(A-16)

Equation (A-8) reads

$$\log K_n = \frac{1}{2}\log\left(\frac{\pi n}{4}\right) + \frac{1}{2}\cdot\frac{1}{n} + \frac{1}{8}\cdot\frac{1}{n} +$$

$$\left[\frac{1}{8}\ \frac{1}{n^2}\ B_n - \frac{1}{12}\left(\frac{1}{\left(1+\frac{1}{n}\right)} - \frac{1}{4}\cdot\frac{1}{\left(1+\frac{1}{2n}\right)}\right)\cdot\frac{1}{n^2} - \left(C_n + C_{n+1} - C_{2n+1}\right)\right]$$

or

$$\log K_n = \frac{1}{2}\log\left(\frac{\pi n}{4}\right) + \frac{5}{8}\cdot\frac{1}{n} + \Delta \qquad \text{(A-17)}$$

The remainder Δ can be estimated:

$$\left|\Delta\right| \leq \frac{1}{n^2}\left[\frac{1}{8}\left|B_n\right| + \frac{1}{12}\left(1+\frac{1}{4}\right)\right] + \left|C_n + C_{n+1} - C_{2n+1}\right|$$

Equations (A-9) and A-14) yield

$$\left|\Delta\right| \leq \frac{1}{n^2}\left\{\frac{1}{8}\cdot\frac{4}{\left(1-\frac{1}{n}\right)} + \frac{5}{48} + \frac{1}{8\pi}\right\} \qquad \text{(A-18)}$$

For $n \geq 10$ we have

$$\left|\Delta\right| \leq \frac{1}{100}\left\{\frac{1}{2\left(1-\frac{1}{10}\right)} + \frac{5}{48}\quad\frac{1}{8\pi}\right\} < \frac{1}{100} \qquad \text{(A-19)}$$

Hence, for $n \geq 10$, $\log K_n$ can be expressed with sufficient accuracy by

$$\log K_n = \frac{1}{2} \log \left(\frac{\pi n}{4} \right) + \frac{5}{8} \cdot \frac{1}{n} \pm 0.01 \qquad \text{(A-20)}$$

Since

$$0 < e^{-0.01} < e^{+0.01} = 1.01005 \ldots < 1.011$$

we obtain the approximation formula

$$K_n \approx \frac{1}{2} \sqrt{\pi n} \; e^{\frac{5}{8} \cdot \frac{1}{n}} \qquad \text{(A-21)}$$

which gives the exact value for K_n within an accuracy of less than 1.1%, if $n \geq 10$. It is clear that K_n tends to infinity like the square root of n.

NASA-Langley, 1966 CR-471